Symposium V, Materials Research Society, San Francisco, CA, April, 2000

Lateral Dye Distribution with Ink-Jet Dye Doping of Polymer Organic Light Emitting Diodes

Conor F. Madigan, Thomas R. Hebner, and J. C. Sturm
Department of Electrical Engineering, Princeton University, Princeton, NJ 08544
Richard A. Register, Sandra Troian
Department of Chemical Engineering, Princeton University, Princeton, NJ 08544

ABSTRACT

In this work we investigate the lateral dye distribution resulting from the dye doping of a thin polymer film by ink-jet printing (IJP) for the integration of color organic light emitting diodes (OLED's). The dye is found to segregate into distinct outer rings following rapid droplet evaporation, while slower evaporation rates are found to significantly reduce (or eliminate) this effect. The dye segregation phenomena are found to depend critically on the mechanisms of droplet evaporation. Good dye uniformity was obtained using a low vapor pressure solvent, and integrated, 250 micron red, green, and blue polymer organic light emitting diodes (OLED's) were fabricated with this technique. These devices had good color uniformity over most of the device area and similar electrical properties to comparable spin-coated devices without IJP.

I. INTRODUCTION

Polymer OLEDs are a promising technology for flat panel displays [1]. These devices typically consist of a multi-layer sandwich of a transparent substrate, a transparent anode (in our work, Indium Tin Oxide), a thin film of an organic polymer blend (in our work, the hole-transporting polymer Poly(N-vinyl carbazole) (PVK) doped with an emissive dye), and a reflecting cathode. (The device structure and principle of operation are illustrated in Fig. 1.) When current is driven through the device, holes from the anode and electrons from the cathode combine in the organic film to form excitons, which emit light as they decay. It has been shown that by doping the organic active layer with a small amount of dye one can tune the emission wavelength [2]. Currently, spin coating is the standard method for depositing a polymer blend film, which produces a uniform layer of polymer. However, this does not allow one to integrate multiple colors onto a single substrate, because the film is the same everywhere.

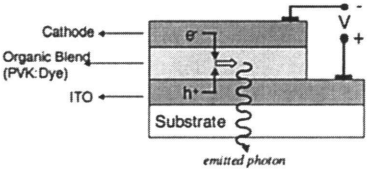

Fig. 1. Basic OLED structure and operation.

It has been proposed previously [3,4] to locally dope an initially undoped PVK film by depositing droplets of a dye solution onto the film surface and allowing the droplet to evaporate. This task is ideally suited to IJP. This basic procedure is outlined schematically in Fig. 2. To integrate red, green, and blue devices onto a single substrate, solutions of red, green, and blue dyes are locally printed onto the same substrate. Our

Mat. Res. Soc. Symp. Proc. Vol. 624 © 2000 Materials Research Society

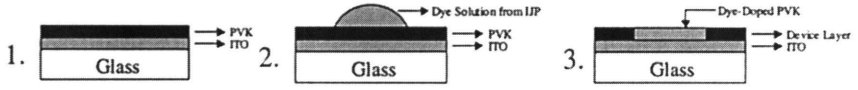

Fig. 2. Procedure for dye-doping by ink jet printing.

objectives in developing this technique are to (a) produce a uniform dye distribution over the device area and film depth and (b) maintain the initial film morphology (so that the electrical device characteristics are not degraded). In employing IJP, this technique should be relatively inexpensive to perform and applicable to large area substrates.

II. IJP DROPLET FORMATION

Our experimental apparatus consists of a piezo-electric type ink jet printer (supplied by MicroDrop GmbH) with a glass print head (which is therefore resistant solvent damage) and x-y-z print head stage motion. In addition, our system has integrated digital imaging equipment, allowing us to view droplet ejection from the print head nozzle directly and to view drying droplets (from above) under high magnification. The print nozzle consists of a 25 μL capillary cavity surrounded by a piezo-electric sleeves which can contract and expand the fluid cavity (see Fig. 3). To drive a droplet out of the nozzle, a first positive then negative pressure pulse is applied to the fluid through the voltages applied to the piezo-electric sleeve. The positive pulse drives the fluid down into the nozzle tip (which is 50 μm in diameter), and if sufficient energy is supplied by this pulse, a droplet (with diameter slightly larger than the nozzle diameter) will be ejected. The essential free parameters for controlling droplet ejection are the piezo voltage and the pulse duration.

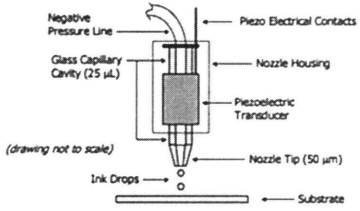

Fig. 3. Schematic of Ink Jet Nozzle. (The negative pressure line is used to balance gravitational forces.)

Several parameters are relevant to understanding droplet formation from an ink jet printer: system geometry (i.e. of capillary cavity and nozzle), properties of the fluid being printed (i.e. viscosity, surface tension, and density), and the relationship between the applied voltage and the resulting pressure pulses. Even each of these parameters is known in detail, a closed-form analysis of the governing Navier-Stokes equations is not possible. However, there is a rapidly growing literature on approximate solutions and numerical simulations of ink-jet flow (e.g. [5-7]), and some important trends are observed.

Droplet formation can be divided up into four regimes, based on the applied voltage. At very low voltages, no droplet is ejected, because the applied pressure pulse has insufficient energy. At higher voltages, single, stable droplet ejection is observed. At still higher voltages, satellite droplets are observed along with the main droplet, and this regime is generally less stable than the single droplet regime. Finally, at yet higher voltages, the ejected fluid will not form into a main droplet and satellites, but break up into an uncontrolled spray, or "jet." These four regimes were clearly demonstrated experimentally on our system with Dimethyl Sulfoxide (DMSO) (see Fig. 4).

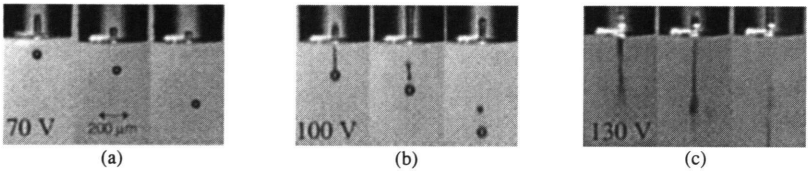

(a) (b) (c)

Fig. 4. Observation of droplet formation regimes with DMSO. No drops were observed for voltages below 60V. (a) Single droplet regime. (b) Satellite droplet regime. (c) "Jet" regime.

We investigated droplet formation with numerous solvents, and found that we could not form droplets (stable or otherwise) at any voltage or pulse duration for solvents with low viscosity and low surface tension on our system. This phenomenon is not reported in the literature. Nevertheless, this introduced a new constraint on solvent selection for our work. The results of our solvent IJP characterization experiments are summarized in Figure 5.

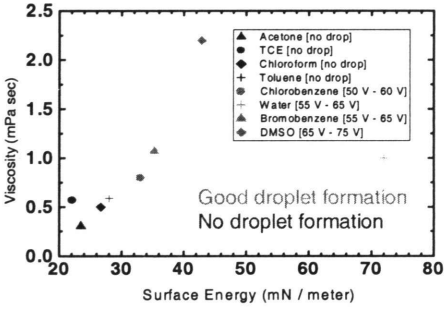

Fig. 5. IJP Solvent Space. For printable solvents, the voltage range for the single droplet regime is given in the legend in brackets.

III. LATERAL DYE DISTRIBUTION

Once a droplet of dye solution is deposited on the polymer film, the actual dye doping occurs over the course of the evaporation of the solvent. Understanding how the dye is laterally distributed in the film, therefore, requires an understanding how the droplet dries. There are essentially two basic types of droplet drying: unpinned and pinned (see Fig. 6).

It is well known that a droplet of fluid on surface has a characteristic contact angle, θ_c, which is dependent primarily on the fluid-surface interface (and only weakly on the surface-air and fluid-air interfaces). In unpinned evaporation, θ_c remains constant as fluid from the droplet surface evaporations, and the droplet radius shrinks correspondingly. In pinned evaporation, the droplet radius remains constant, and instead θ_c shrinks. Though the phenomenon of pinning is not fundamentally understood, it has been proposed that it is the result of surface roughness (including possible "self-roughening" by solute deposition) [8-10]. In addition, it is believed that for the droplet

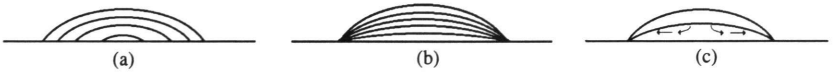

(a) (b) (c)

Fig. 6. Evaporation phenomena. (a) Unpinned. (b) Pinned. (c) Flow during pinned evaporation.

radius to remain constant during evaporation, fluid must flow out from the center to the edge of the drop, leading to a possible mass flow of solute towards the edges [8], as illustrated schematically in Fig. 6c.

Our first dye doping experiments were performed on ~100 nm PVK films, using a solution of the green emitting dye Coumarin 6 (C6) in acetone. Since we could not print acetone with our ink-jet printer, in these experiments we used a syringe to deposit individual droplets of ~11μL, which had a deposited radius of ~7mm. We found that for room temperature evaporation, the acetone droplet remained pinned at its initial radius for ~35 s, and then its radius fell rapidly during the remaining 15 s of evaporation (see Fig. 7a). The resulting dye distribution was observed under ultraviolet (UV) photoluminescence (PL) (see Fig. 7b), and revealed distinct rings of high dye concentration corresponding to droplet pinning, while between the rings, the dye concentration was very low. This observation of dye pile-up into rings was further confirmed by X-ray microprobe. These results clearly demonstrated that mass transport of solute from the center of the droplet to the edges (through some mechanism) occurred. Reducing the evaporation rate by cooling the substrate to 4°C greatly improved the dye distribution uniformity over the droplet area; however, substantial segregation of dye towards the edges was still clearly observed.

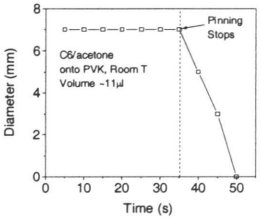

(a)

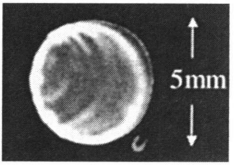

(b)

Fig. 7. Acetone:C6 Deposition. (a) Droplet radius with time during evaporation. (b) Photoluminescence of dye doping, where brightness corresponds to C6 concentration.

Many solvents were considered when determining the best choice for our initial IJP experiments. Essentially, we required a *printable* solvent that dissolved the dye and not the PVK films we would be printing on. In addition, because our work with acetone suggested that slower evaporation times would improve the dye distribution, we desired a solvent with a low vapor pressure. Among the common solvents we tried, DMSO was the only one to meet all these requirements (see Table I).

Table I. Solvents Investigated for IJP Dye Doping Candidacy. (All values for 25°C.)

Name	Formula	Viscosity* (η) (mPa·s)	Surface Energy* (γ) (mN/m)	Vapor Pressure* (p_v) (kPa)	Dissolves Dyes	Dissolves PVK	Prints
Chlorobenzene	C_6H_5Cl	0.753	32.99	1.6	Yes	Yes	Yes
Cyclohexanone	$C_6H_{10}O$	2.02	34.57	0.53	Yes	Yes	Yes
Tetrachloroethane	$C_2H_2C_{l4}$	1.84	35.58	1.6	Yes	Yes	Yes
Dimethyl sulfoxide	**C_2H_6SO**	**2.20**	**42.92**	**0.08**	**Yes**	**No**	**Yes**
Water	H_2O	1.00	71.99	1.00	No	No	Yes
Chloroform	$CHCl_3$	0.58	26.67	26	Yes	Yes	No
Acetone	C_3H_6O	0.30	23.46	31	Yes	No	No

We printed droplets of C6 in DMSO onto PVK films, and observed the drying phenomena. We found that the droplet was pinned for the first 600 s, and for the remaining 400 s evaporation proceeded through a complex sequence of pinning and

slipping (see Fig. 8a). The resulting dye distribution was observed using a PL image of the droplet, which revealed a fairly uniform dye distribution, but with a noticeable segregation of dye towards the center (see Fig. 8b). There were no high concentration outer rings observed as in the acetone results. Closer inspection of the PL image shows that instead, a small number of thick, circular bands of uniform dye distribution are present around an essentially uniform central region, with increasing dye concentration towards the center. The edges of these regions correspond well to the pinned radii observed during evaporation, suggesting that in a region of PVK suddenly exposed by a droplet slip, the absorbed solvent evaporates without any dye redistribution. This is consistent with the assumption that the evaporation of the solvent absorbed into the ~100 nm film should occur extremely rapidly and evenly over the exposed film area. (This result also suggests that in the PVK *under* the solvent droplet, the dye concentration is uniform at the time of the slip.)

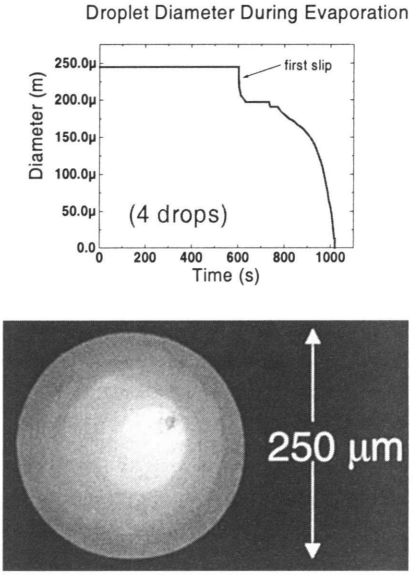

(b)

Fig. 8. DMSO:C6 IJP Deposition.
(a) Droplet radius with time during evaporation.
(b) Photoluminescence of dye doping.

We fabricated integrated red, green, and blue electrical devices on a single substrate, using the dyes Nile Red, C6, and Coumarin 47 to produce each respective color. The resulting 250 μm devices demonstrated similar electrical characteristics to spin-coated devices without IJP, suggesting that the IJP dye doping process did not adversely affect the electrical behavior of the PVK film. The observed electroluminescence (EL) was investigated for uniformity, and an image of a characteristic device is given in Fig. 9. The color uniformity is good over most of the device area, however, there is a distinct dark spot observed in the center of the device, with a slight darkening of the luminance just around this spot. The increased dye concentration in the center of the device (observed in the PL results) could explain a darkening of the luminance (due to dye concentration quenching [11]) in the center, but this effect cannot explain the sharp,

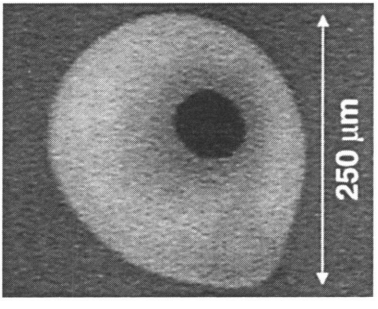

Fig. 9. Electroluminescence of IJP dye doped OLED.

completely dark spot observed. This dark spots appears to be correlated with the surface deposition of some material during the extremely fast drying which occurs in the last stages of the evaporation process over a total region with a radius of about 20 microns, but the details are still unknown.

IV. SUMMARY

We have developed a system to investigate the dye doping by IJP of polymer OLED's, including a highly controllable all-glass ink jet printer and digital imaging equipment for studying IJP droplet formation and droplet drying phenomena. Using a very low vapor pressure solvent, uniform dye distribution over the droplet area was achieved. The dye distribution is critically affected by the dynamics of the drying process, which at present are only qualitatively understood. Integrated 250-micron RGB devices were demonstrated with good color uniformity and with electrical properties comparable to spin-coated devices without IJP.

V. ACKNOWLEDGEMENTS

This work was supported by DARPA/AFOSR, NSF, and NJCST. The authors would also like to thank Joe Goodhouse for his expert assistance in obtaining PL images.

VI. REFERENCES

[1] J.H. Burroughs, D.D.C. Bradley, A.R. Brown, R.N. Marks, K. Mackay, R.H. Friend, P.L. Burns, A.B. Holmes, Nature **347**, 539 (1990).
[2] J. Kido, M. Kohda, K. Okuyama, K. Nagai, Appl. Phys. Lett. **61**, 761 (1992).
[3] T.A. Hebner, J.C. Sturm, APL **73**, 1775 (1998).
[4] C.L. Chang, L.P. Rokhinson, J.C. Sturm, Appl. Phys. Lett. **73**, 3568 (1998).
[5] E.D. Wilkes, S.D. Phillips, O.A. Basaran, Phys. of Fluids **11**, 3577 (1999).
[6] X.G. Zhang, J. Coll. Int. Sci. **212**, 107 (1999).
[7] T.W. Shield, D. B. Bogy, F.E. Talke, IBM J. Res. Dev. **31**, 96 (1987).
[8] R.D. Deegan, Phys. Rev. E **61**, 475 (2000).
[9] E. Adachi, A.S. Dimitrov, K. Nagayama, Langmuir **11**, 1057 (1995).
[10] P.G. de Gennes, Revs. Mod. Phys. **57**, 827 (1985).
[11] C.C. Wu, J.C. Sturm, R.A. Register, J. Tian, E.P. Dana, M.E. Thompson, IEEE Trans. on Elec. Dev. **44**, 1269 (1997).